J Radioanal Nucl Chem (2012) 292:705–710
DOI 10.1007/s10967-011-1481-4

^{99m}Tc–meropenem as a potential SPECT imaging probe for tumor hypoxia

T. M. Sakr · M. A. Motaleb · I. T. Ibrahim

Received: 29 September 2011 / Published online: 19 October 2011

Abstract Meropenem was successfully radiolabeled with ^{99m}Tc in high labeling yield ($92 \pm 2\%$) and stability (~ 6 h). ^{99m}Tc–meropenem showed high accumulation in tumor hypoxic tissue (4.193% injected dose/g organ). ^{99m}Tc–meropenem showed high ability to differentiate the tumor tissue from inflamed or infected tissues in different mice models as its T/NT ratio ~ 4 in case of tumor mice model while T/NT ratio ~ 1 in case of inflamed mice model. So, ^{99m}Tc–meropenem showed high selectivity in comparison with FDG-PET and ^{99m}Tc-nitroimidazole analogues. Thus, ^{99m}Tc–meropenem could be used as a selective potential imaging agent for diagnosis of tumor hypoxia.

Keywords Meropenem · ^{99m}Tc · SPECT · Tumor · Imaging · Hypoxia

Introduction

Nuclear oncology, as a tool for tumor imaging [e.g. Single Photon Emission Computed Tomography (SPECT) and Positron Emission Tomography (PET)], is the medical branch which involves a large variety of procedures to assess patients with already-known or unspecified neoplastic conditions [1]. The differences of the pathological and physiological processes between the tumor cells and the normal ones allow the differentiation of the tumor tissue from the normal tissue [2, 3]. Tumor imaging techniques depend on the approach of developing specific radiopharmaceuticals able to target the radiotracer to the specified tumor tissues with high T/NT ratios showing high selectivity and specificity [4]. Tumor hypoxia is a pathological condition in which tumor cells lack the oxygen required for their normal metabolic pathways [5, 6], and it occurs when the size of a tumor increases to a range disrupting the balance between supply and consumption of oxygen in the area. Up to 50–60% of the advanced solid tumors may exhibit hypoxic tissue areas due to the rapid proliferation and vascular abnormalities [5–7]. Hypoxia represents a basic role for the tumor resistance for radiotherapy. The development of noninvasive imaging radiopharmaceutical targeted to tumor hypoxia represents a solution for the wide limitation of the invasive methods to measure hypoxia. In the development of hypoxia imaging agent, nitroimidazole analogues, which are enzymatically reduced and accumulated in hypoxic regions, have received great attention as hypoxia imaging agents. Several ^{99m}Tc labeled nitroimidazole analogues have been reported, however they showed some defects like, lower tumor uptakes and slow blood clearance [8–13]. Currently, ^{18}F-fluoromisonidazole ([^{18}F] FMISO) has been used to evaluate tumor hypoxia [14, 15]. However, the short half life and high cost of the [^{18}F] isotope restrict its wide application in clinical nuclear medicine. Differentiation between tumor and inflammation is the main fundamental unsolved problem in the staging of malignant tumors [16, 17]. The well recognized limitation of FDG-PET, which gives rise to false positive results, is the high uptake of FDG in human [16–18] and experimental inflammatory lesions [19–26]. Therefore, tumor imaging tracers are required that accumulate exclusively in tumor cells [27].

T. M. Sakr (✉)
Radioactive Isotopes and Generator Department, Hot Labs Center, Atomic Energy Authority, P.O. Box 13759, Cairo, Egypt
e-mail: Tamer_sakr78@yahoo.com

M. A. Motaleb · I. T. Ibrahim
Labeled Compounds Department, Hot Labs Center, Atomic Energy Authority, P.O. Box 13759, Cairo, Egypt

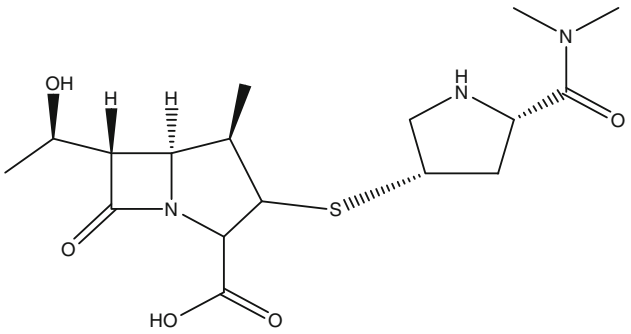

Fig. 1 Meropenem chemical structure

Meropenem, Fig. 1, is a beta-lactam carbapenem antibiotic for parenteral use which exerts bactericidal action by interfering with vital bacterial cell wall synthesis and it penetrates well into many tissues and body fluids [28]. This work aims to label meropenem with ^{99m}Tc under different experimental conditions and investigation of the potential use of ^{99m}Tc–meropenem (prepared under the optimum conditions) as a potential SPECT probe for tumor hypoxia, using a mouse model.

Experimental

All of the chemical reagents were of AR grade and bidistilled water was used for solution preparation. Meropenem was obtained as a gift from Astra Zeneca Company. Albino mice, each of 20–25 g, were used for the biological distribution study. A NaI(Tl) γ-ray scintillation counter (Scaler Ratemeter SR7 model, England) was used for the measurement of γ-ray radioactivity. A HPLC (Hitachi model, Alphabond C18 125A 10U column with I.D. 3.9 and length 300 mm, Japan) was used to analyze the purity of the prepared ^{99m}Tc–meropenem. ^{99m}Tc was eluted as $^{99m}TcO_4^-$ from ^{99m}Mo/^{99m}Tc generator (radionuclidic purity: 99.99%, radiochemical purity: 99.99%, activity: 1 Ci, Elutec Brussels, Belgium).

Preparation of ^{99m}Tc–meropenem complex

Labeling procedure

Exactly weight 3 mg amounts of meropenem, dissolved in 1 mL N_2-purged distilled water, were separately transferred to evacuated penicillin vials. Then, 1 mL of phosphonate buffer at different pH ranging from 3 to 9.5 were added. Exactly 4 μg of $SnCl_2{\cdot}2H_2O$ were added to each vial followed by 1 ml of freshly eluted $^{99m}TcO_4^-$ (400 MBq) was added to each vial. The reaction mixtures were left at room temperature for 5 min. The same procedure was repeated with varying $SnCl_2{\cdot}2H_2O$ amounts (4–100 μg), varying meropenem amounts (1–15 mg), and different reaction times (1–240 min).

Radiochemical purity of ^{99m}Tc–meropenem complex

The radiochemical purity, percent labeling yield, of the labeled ^{99m}Tc–meropenem complex was determined by using ascending paper chromatographic technique and HPLC. Strips of Whatman No. 1 paper chromatography of 13 cm long and 0.5 cm wide were marked at a distance of 2 cm from the lower end and lined into sections 1 cm each up to 10 cm. A spot from ^{99m}Tc–meropenem complex solution was applied using hypodermic syringe, and then the strip was developed in an ascending manner in a closed jar filled with N_2 gas. The developing solvents were acetone for developing one paper and a mixture of ethanol:water:ammonium hydroxide (2:5:1) for developing a duplicate paper strip. After complete development, the strips were dried and cut into fragments 1 cm each. Then the sections were assayed in a NaI(Tl) γ-ray scintillation counter.

The HPLC analysis of ^{99m}Tc–meropenem complex was done by injection of 10 μL ^{99m}Tc–meropenem complex, after 0.22 μm Millipore filtration, into the column (RP-18. 300 × 3.9 mm^2, Alphabond) and UV spectrophotometer detector (SPD-6A) which was adjusted to the 270 nm wavelength. The column was eluted with mobile phase (acetonitrile: 0.05 M phosphate buffer pH 7: H_2O mixture in ratio 30:5:65) and the flow rate was adjusted to 1 mL/min [29]. Fractions of 1 mL were collected separately using a fraction collector up to 20 and counted in a well-type NaI(Tl) detector connected to a single channel analyzer.

In vitro stability of ^{99m}Tc–meropenem complex

The in vitro stability of ^{99m}Tc–meropenem complex was investigated as a function of time up to 6 h post labeling.

Biodistribution study

The study was approved by the animal ethics committee, Labeled Compound Department, and was in accordance with the guidelines set out by the Egyptian Atomic Energy Authority. Target organ uptake of ^{99m}Tc–meropenem complex was evaluated in male Albino Swiss mice weighing 20–25 g. A volume of 0.1 mL of ^{99m}Tc–meropenem complex containing 185–1850 kBq was intravenously injected in the tail vein of mice. The animals were anesthetized by chloroform at the predesigned time interval and their body organs and fluids were separated, weighted and their radioactivities were assayed using a NaI(Tl) γ-ray scintillation counter. Biological distribution of

^{99m}Tc–meropenem complex in mice organs and fluids was studied as a function of time, 20, 60 and 100 min post injection. The percentages of the injected dose/g organ or fluids were calculated. Differences in the data were evaluated with the Student *t* test. Results for *P* using the 2-tailed test are reported and all the results are given as mean ± SEM. The level of significance was set at $P < 0.05$.

These procedures were performed on three different mice models where T/NT ratio are calculated and compared.

Tumor hypoxia bearing mice model

The parent tumor line (Ehrlich Ascites Carcinoma) was withdrawn from 7 days old donor female Swiss Albino mice and diluted with sterile physiological saline solution to give 12.5×10^6 cells/mL. Exactly 0.2 mL solution was then injected intramuscularly in the right thigh to produce a solid tumor. The animals were maintained till the tumor development was apparent (10–15 day).

Bacterial infection bearing mice model

Induction of infectious foci in mice was induced as follow: A single clinical isolation of *Escherichia coli* (*E. coli*) from biological samples were used to produce focal infection. Individual colonies were diluted in order to obtain turbid suspension. Groups of three mice were intramuscularly injected with 200 µL of the suspension in the left lateral thigh muscle [30–32]. Then, the mice were left for 24 h to get a gross swelling in the infected thigh.

Sterile inflammation bearing mice model

Sterile inflammation was induced by injecting 200 µL of turpentine oil [32, 33], sterilized by autoclaving at 121 °C for 20 min, intramuscularly in the left lateral thigh muscle of the mice. Two days later, swelling appeared.

Results and discussion

Radiochemical purity of ^{99m}Tc–meropenem complex

The radiochemical purity, percent labeling yield, of the prepared ^{99m}Tc–meropenem complex was checked by two chromatographic techniques.

1. Ascending paper chromatographic technique, using acetone as a developing solvent where free $^{99m}TcO_4^-$ was moved with the solvent front ($R_f = 1$) while other species (reduced hydrolyzed-^{99m}Tc colloid and ^{99m}Tc–meropenem complex) remained at the point of spotting. When a mixture of ethanol: water: ammonium hydroxide (2:5:1) was used as a developing solvent, reduced hydrolyzed-^{99m}Tc colloid remained at the origin ($R_f = 0$) while free $^{99m}TcO_4^-$ and ^{99m}Tc–meropenem complex migrate to the top of the paper.

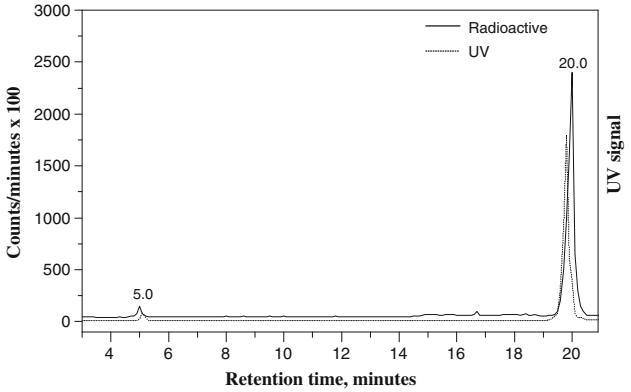

Fig. 2 HPLC radiochromatogram of ^{99m}Tc–meropenem complex

The percent of ^{99m}Tc–meropenem complex was determined as follows:

$$\%\,\text{Labeling yield} = 100 - \left(\%\,\text{Free}^{99m}\text{TcO}_4^- + \%\,\text{Reduced hydrolyzed} - {}^{99m}\text{Tc colloid}\right)$$

2. An HPLC radiochromatogram (Fig. 2) showed two peaks, one at fraction number 5, which corresponds to $^{99m}TcO_4^-$, while the second peak was collected at fraction number 20 which corresponds to ^{99m}Tc–meropenem complex, which was found to coincide with the UV signal. Nearly, 98% of the injected activity in the HPLC was recovered as collected activity.

Effect of pH of the reaction medium

Figure 3 clearly shows that, the pH is critical factor for the formation of the ^{99m}Tc–meropenem complex and the maximum labeling yield of ^{99m}Tc–meropenem complex (92 ± 2%) was obtained at pH value equal to 9.

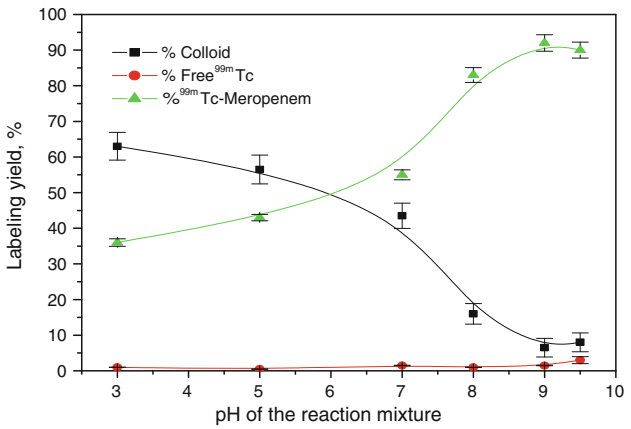

Fig. 3 Effect of pH of the reaction medium on the percent labeling yield of ^{99m}Tc–meropenem complex

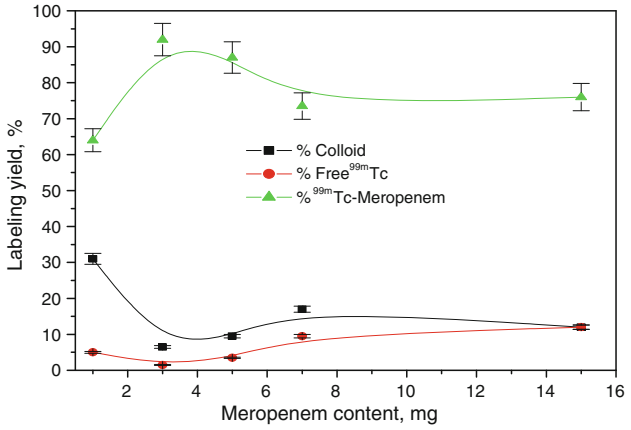

Fig. 4 Effect of meropenem content on the formation of ^{99m}Tc–meropenem complex

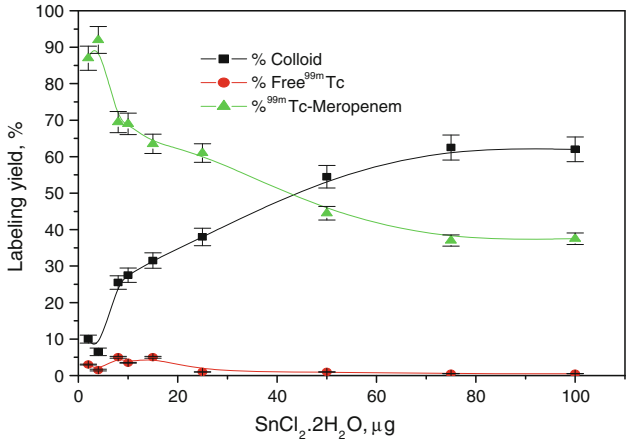

Fig. 5 Effect of $SnCl_2{\cdot}2H_2O$ content on the formation of ^{99m}Tc–meropenem complex

Effect of meropenem content

Meropenem content ranging from 1 to 15 mg was studied as shown in Fig. 4. At 1 mg meropenem, low percent labeling yield (64%) was obtained which increased with the increasing of the meropenem content till reach its highest yield (92 ± 2%) at 3 mg meropenem. Increasing the meropenem content beyond to 3 mg, the labeling yield decreased.

Effect of $SnCl_2{\cdot}2H_2O$ content

The $SnCl_2{\cdot}2H_2O$ content, in the range of 4–100 µg, was investigated affecting the percent labeling yield of the ^{99m}Tc–meropenem complex as shown in Fig. 5. At $SnCl_2{\cdot}2H_2O$ content 4 µg, the maximum labeling yield (92 ± 2%) was obtained. By increasing the $SnCl_2{\cdot}2H_2O$ content up to 100 µg, the percent labeling yields were decreased extensively. This may be due to the fact that most of the ligand molecules were consumed in the formation of complexes, so the pertechnetate is reduced to insoluble technetium (IV) $TcO_2{\cdot}xH_2O$ in the absence of ligand [34] or due to the fact that the excess amount of stannous chloride leads to the formation of stannous hydroxide colloid $Sn(OH)_3$ (62 ± 1.1% at 100 µg $SnCl_2{\cdot}2H_2O$) in basic medium [35]. So, the optimum amount of $SnCl_2{\cdot}2H_2O$ content required for the formation of ^{99m}Tc–meropenem complex was 4 µg.

Effect of reaction time

The formation of ^{99m}Tc–meropenem complex was relatively fast as the maximum labeling yield was obtained at 5 min and remained constant up to 1 h.

So, by studying all the factors affecting the labeling yield of ^{99m}Tc–meropenem starting from meropenem amount, $SnCl_2{\cdot}2H_2O$ content, pH and time, it was found that the highest labeling yield (92 ± 2%) was formed with 3 mg meropenem and 4 µg $SnCl_2{\cdot}2H_2O$ at pH 9 after 5 min reaction time.

In vitro stability of ^{99m}Tc–meropenem complex

The in vitro stability results of ^{99m}Tc–meropenem complex indicated that the labeled product remained nearly stable for more than 6 h after labeling.

Biodistribution study

Figure 6 shows the T/NT ratios of the three induced states in mice at different time intervals. This figure approve that ^{99m}Tc–meropenem is a very selective and specific tumor hypoxia imaging agent able to differentiate between different clinically manifested cases like infection or inflammation and the tumor which already cleared by the T/NT ratios of both of the bacterial infection and the inflammation as that their T/NT ratios ~1 at all time intervals while in case of the tumor hypoxia case it reaches high T/NT ratio ~4 at 60 min. This approach shows that ^{99m}Tc–meropenem is highly advance than FDG-PET which gives rise to false positive results in experimental inflammatory lesions [16–26].

Table 1 represents the biological distribution of ^{99m}Tc–meropenem in tumor hypoxia bearing mice model showing the % accumulation in body organs and fluids expressed as % injected dose/g organ (fluid) (% ID/g). The high activity of both of the liver and kidneys approves that the ^{99m}Tc–meropenem excretion is through the two pathways renally and hepatobilliary. The high percent tumor

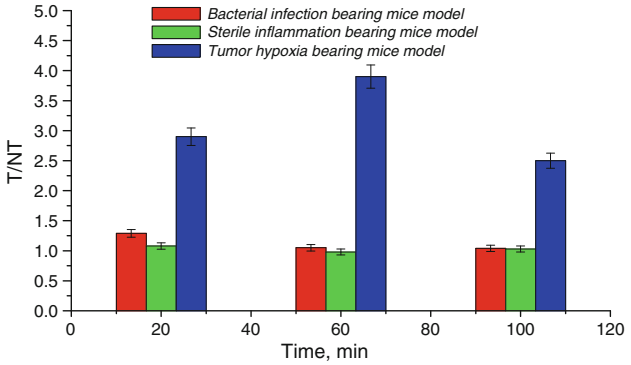

Fig. 6 T/NT ratios of ^{99m}Tc–meropenem complex in different mice models as a function of time

Table 1 Biological distribution of ^{99m}Tc–meropenem complex in mice as a function of time

Body organ (fluid)	% Injected dose/g organ (fluid) at time intervals		
	20 min	60 min	100 min
Tumor hypoxic muscle	2.161 ± 0.04	3.483 ± 0.06	4.193 ± 0.08
Normal muscle	0.7453 ± 0.01	0.8931 ± 0.02	1.676 ± 0.03
Kidneys	6.302 ± 0.02	9.968 ± 0.39	11.67 ± 0.53
Liver	4.45 ± 0.09	5.575 ± 0.11	3.513 ± 0.07
Blood	6.203 ± 0.15	5.393 ± 0.17	3.636 ± 0.12
Heart	1.449 ± 0.07	1.691 ± 0.08	0.631 ± 0.03
Lungs	1.462 ± 0.07	1.844 ± 0.09	1.049 ± 0.04
Bone	1.295 ± 0.06	1.792 ± 0.09	2.048 ± 0.1
Spleen	0.698 ± 0.04	0.805 ± 0.04	0.458 ± 0.02
Intestine	1.57 ± 0.03	2.559 ± 0.05	1.784 ± 0.03
Stomach	0.514 ± 0.01	0.728 ± 0.02	0.347 ± 0.03

Mean ± SD (mean of five experiments)

hypoxia uptake of ^{99m}Tc–meropenem (4.193 at 100 min) shows high affinity to the tumor tissue if compared with different tumor imaging agents like ^{99m}Tc(CO)$_3$-VIP and ^{99m}Tc–polyamine analogues which showed percent tumor hypoxia uptake ranging from 0.5 to 1 [36–38].

Conclusion

^{99m}Tc–meropenem represents a potential tumor hypoxia imaging agent able to overcome two main problems of the commonly used agents, as it highly accumulates in the tumor cells showing %ID/g 4.193 and has a very powerful ability to differentiate between inflamed or infected tissues from the tumor tissues showing T/NT ratio ~4. So, this paper can implement new potential specific and selective tumor hypoxia imaging agent which is ^{99m}Tc–meropenem.

References

1. Fukunoto M (2004) Ann Nucl Med 18(2):79
2. Schottelius M, Wester H (2009) Methods 48:161
3. André Lues BB, Luciene GM, Carolina AF, Mônica CO, Alfredo MG, Valbert NC (2010) Bioorg Med Chem Lett 20:6182
4. Santos-Cuevas CL, Ferro-Flores G, Murphy CA, Ramerez F, Luna-Gutiérrez MA, Pedraza-Lopez M, Garcea-Becerra R, Ordaz-Rosado D (2009) Int J Pharm 375:75
5. Vaupel P, Mayer A (2007) Cancer Metastasis Rev 26:225
6. Xilin S, Gang N, Nicholas C, Baozhong S, Xiaoyuan C (2010) Mol Imaging Biol 13(3):399
7. Hu M, Polyak K (2008) Curr Opin Genet Dev 18:27
8. Chu TW, Li RJ, Hu SW, Liu XQ, Wang XY (2004) Nucl Med Biol 31:199
9. Kong DJ, Lu J, Ye SZ, Wang XB (2007) J Label Compd Radiopharm 50:1137
10. Mallia MB, Mathur A, Subramanian S, Banerjee S, Sarma HD, Venkatesh M (2005) Bioorg Med Chem Lett 15:3398
11. Mallia MB, Subramanian S, Banerjee S, Sarma HD, Venkatesh M (2006) Bioorg Med Chem 14:7666
12. Mallia MB, Subramanian S, Mathur A, Sarma HD, Venkatesh M, Banerjee S (2008) Bioorg Med Chem Lett 18:5233
13. Zhang Y, Chu TW, Gao XG, Liu XQ, Yang Z, Guo ZQ, Wang XY (2006) Bioorg Med Chem Lett 16:1831
14. Yang DJ, Wallace S, Cherif A, Li C, Gretzer MB, Kim EE, Podoloff DA (1995) Radiology 194:795
15. Junbo Z, Qian Y, Jinfeng H, Yan P, Sheng Y, Yining H, Tingting T, Chenchen Y, Xuebin W (2010) J Radioanal Nucl Chem 283:481
16. Larson SM (1994) J Nucl Med 35:1653
17. Barbara S, Ursula T, Michael H, Christof S, Markus S, Reingard SS (2006) Eur J Nucl Med Mol Imaging 33:932
18. Bakheet SM, Powe J (1998) Semin Nucl Med 28:352
19. Kubota R, Yamada S, Kubota K, Ishiwata K, Tamahashi N, Ido T (1992) J Nucl Med 33:1972
20. Kubota K, Kubota R, Yamada S, Tada M (1995) Nucl Med Biol 22:193
21. Kubota R, Kubota K, Yamada S, Tada M, Iwata R, Tamahashi N (1995) J Nucl Med 36:484
22. Yamada S, Kubota K, Kubota R, Ido T, Tamahashi N (1995) J Nucl Med 36:1301
23. Sugawara Y, Gutowski TD, Fisher SJ, Brown R, Wahl RL (1999) Eur J Nucl Med 26:333
24. Reinhardt MJ, Kubota K, Yamada S, Iwata R, Yaegashi H (1997) J Nucl Med 38:280
25. Gutowski TD, Fisher SJ, Moon R, Wahl RL (1992) J Nucl Med 33:925
26. Wahl RL, Fisher SJ (1993) J Nucl Med 34:104
27. Heiss P, Mayer S, Herz M, Wester HJ, Schwaiger M, Senekowitsch-Schmidtke R (1999) J Nucl Med 40:1367
28. Bilgrami I, Roberts JA, Wallis SC, Thomas J, Davis J, Fowler S, Goldrick PB, Lipman (2010) J Antimicrob Agents Chemother 54(7):2974
29. El Shaboury SR, Saleh GA, Mohamed FA, Rageh AH (2007) J Pharm Biomed Anal 45:1
30. Van Der Laken CJ, Boerman OC, Oyen WJG, Van Der Ven MTP, Van Der Meer JWM, Corstens FHM (2000) J Nucl Med 41:463
31. Oyen WJG, Boerman OC, Corstens FHM (2001) J Microbiol Methods 47:151
32. Mostafa M, Motaleb MA, Sakr TM (2010) Appl Radiat Isot 68:1959

33. Asikoglu M, Yurt F, Cagliyan O, Unak P, Ozkilic H (2000) Appl Radiat Isot 53:411
34. Srivastava SC, Richards P (1983) In: Rayudu GVS (ed) Radiotracers for medical applications. CRC series in radiotracers in biology and medicine. CRC Press, Boca Raton, p 107
35. Wardell JL (1994) In: King RB (ed) Encyclopedia of inorganic chemistry, vol 8. Wiley, New York, p 4159
36. Kanchan K, Sudhanand P, Aruna K, Archana M, Archana M, Manu J, Meera V, Ambikalmajan MRP, Rama M, Natesan R (2007) Appl Radiat Isot 65:382
37. Chiara DP, Alan CP, Sotiris M (2009) Nucl Med Biol 36:703
38. Wei-Xing W, Min Y, Shang-Ren P, Chun-Jing Y, Na-Jing W (2008) Drug Dev Res 69:520